Nanotechnology Perceptions
ISSN 1660-6795
www.nano-ntp.com

Combining in Silico, in Vitro Studies to Evaluate Potential De Novo Drug for Covid-19-Associated Coagulopathy from Bambusa Bambos Leaves

Jeyavenkatesh J[1], Muthukumar N J[2], Savariraj Sahayam C[3], Roja Ramani S[4], Melinda Grace Rossan Mathews[5], Shanmuga Priya R[6]

[1]BSMS, MD, PhD, Corresponding author, Head (Medical and Research), Kokila Siddha Hospital and Research Centre, Madurai, jeyavenkateshdrs@gmail.com
[2]Director General, Central Council for Research in Siddha, Chennai, Tamilnadu ccrschennai@gmail.com
[3]PhD, Asst Professor III, Centre for Advanced Research in Indian Systems of Medicine, SASTRA Deemed University, Thanjavur, drsagay@gmail.com
[4]Asst. Medical Officer (Siddha), Govt. Primary Health Centre, Poovanthi, Sivagangai, rojaramanidr@gmail.com, Mobile: 9003000250
[5]Regeneration and Stem Cell Biology, Centre for Molecular and Nanomedical Sciences, Sathyabama Institute of Science and Technology, Chennai, melindagrace.r.cmns@sathyabama.ac.in
[6]Public Health Specialist, National Institute of Siddha, Chennai, Tamilnadu, priyaaram69@gmail.com

SARS-CoV-2 disease is caused by to Coronavirus (COVID-19) which leads to severe mortality in millions of populations around the world. COVID-19 primarily affects the respiratory system and also causes thrombo-inflammatory conditions, and coagulopathies including DVT, PE, PVD, strokes, and cerebral hemorrhages. Thus, thromboprophylaxis is the first line of treatment to be considered in all COVID-19 patients to treat thrombosis, opportunistic infections, inflammation, and as well as COVID-19. Bambusa bambos is a therapeutically important plant in Siddha traditional medicine that has anti-inflammatory, antioxidant, gastric, antispasmodic, and astringent properties. Thus, this work aimed to investigate the thrombolytic potential of the plant to develop a de novo drug model in silico for COVID-19-associated coagulopathy and to standardize it using advanced methods. Microscopical examination revealed the presence of general plant anatomy with the epidermis, cuticle, vascular tissues, and lower epidermis which contained lignin, alkaloids, phenols, and cutin. Particle size morphology and size were analyzed using SEM and Zeta analysis which revealed that the leaf powder contained small irregular particles with smooth surfaces with a zeta potential value of -17.9 indicating the powder particles were stable without aggregation. DNA barcoding analysis of the powder indicated that the tested material was not contaminated by proteins or other polysaccharides. Preliminary phytochemical screening revealed the presence of flavonoids,

phenols, sterols, and tannins in the methanol extract of the plant leaves. Quantitative analysis showed that the extract contained 7.2% of total flavonoids, 7.4% of total phenols, and 0.36% of total tannins. HPTLC fingerprinting analysis revealed the presence of the standard drug, Quercetin in the extract at an Rf value corresponding to 0.61 along with 10 other compounds. GC-MS analysis identified 33 compounds, majorly Diisooctyl phthalate, 3, 7, 11, 15-Tetramethyl-2-hexadecen-1-ol, alpha-Cubebene, and Dibutyl phthalate as major chemical constituents alongside Squalene, Pentadecanoic acid, Neophytadiene, Benzyl Benzoate and 2-methyl-Octacosane. The extract showed potent antibacterial activity against S. marcescens, B. subtilis, P. aeruginosa, E. faecalis, S. aureus, E. coli compared to standard, Amphotericin B and potent antifungal activity against C. albicans and A. niger. The extract showed potent antioxidant activity compared to ascorbic acid in the DPPH assay with IC50 of 59.6 and 8.95 µg/mL respectively. The MTT assay on the HaCaT cell lines indicated that the extract was relatively safer till 100 µg/mL where IC50 was 64.35 µg/mL and showed over 33% better wound healing activity in scratch assay compared to the control group. A potent anticoagulant activity was exhibited by the extract by increasing the clotting time by 2.6 times, prothrombin time by 7.5 times, and % thrombolysis of 68.7% compared to control on chicken blood. Molecular docking studies on 16 compounds selected from GC-MS showed better interaction and binding with Antithrombin III (PDB ID: 2B4X), Thrombin (PDB ID: 1KTS), Factor X (PDB ID: 1KSN) and Vitamin-K epoxide reductase (PDB ID: 3KP9) receptors compared to standard drugs clopidogrel, taxiphyllin, rivaroxaban and warfarin respectively. Out of the 5 De novo models of drugs, model 5 showed a better affinity with the receptors with promising binding energies compared to respective standard drugs. Thus, this research shows that the extract of Bambusa bambos be effectively used to treat thrombosis or thromboembolism and also fight the infections that commonly occur in COVID-19. Further research should be focused on isolating the lead molecule and conducting clinical trials to establish it as a drug of choice for thromboprophylaxis in COVID-19 treatment.

Keywords: COVID-19, Bambusa, Anticoagulant, chicken blood, molecular docking, De novo modelling.

1. Introduction

Severe Acute Respiratory Syndrome Coronavirus Type 2 (SARS-CoV-2) infection is the cause of Coronavirus Disease 2019 (COVID-19). Although the condition primarily affects the respiratory system, it typically affects other organs in varied degrees of severity, from mild to severe, and it may even be fatal.[1] The primary direct causes of death are suppurating lung infection-induced multi-organ failure and septic shock.[2] COVID-19 infection in most cases is featured by thrombo-inflammatory symptoms termed COVID-associated coagulopathy.[3] The disease is associated with an increased prevalence of venous thromboembolism (VTE), deep vein thrombosis (DVT), and pulmonary embolism (PE), resulting in ischemic strokes and peripheral vascular diseases (PVD) also increased cerebral haemorrhages.[4] In COVID-19 patients, the history of malignancy, elevated D-dimer, and duration of hospital stay had a direct and strong correlation to the risk of DVT.[5] Studies conducted on the corpses of COVID-19 patients showed deep vein thrombosis (DVT) in 7.7% and pulmonary embolism (PE) in 23.1% of the patients which indicated that severe PE was the direct cause for the mortality in 1/3rd of the patients. [2] [6] Another study revealed that thrombotic events were frequent in COVID-19 patients which led to cerebral sinus thrombosis resulting in the mortality of 26.6% of the cases.[7]

Thrombosis is the result of inflammation in the vascular endothelium due to viral infection.[8] Thrombosis is caused due to Disseminated Intravascular Coagulation (DIC) by activation of

the coagulation pathway and platelet-fibrin thrombus deposition[9], activation of macrophages, activation of cytokines, overstimulation of renin-angiotensin.[10] Studies showed that changes in prothrombin time (PT) and activated partial thromboplastin time (aPTT) were observed in COVID-19 patients, thus confirming thrombosis is one of the major effects of COVID-19 other than respiratory complications.[11] This signifies an urgent need for the implementation of thromboprophylaxis procedures in COVID-19 patients to lower the risk of thromboembolism and resultant mortality. Further, optimal dosing of anticoagulants is also essential to improve overall therapeutic results in COVID-19 patients.[12]

Even though the existing medications are effective for treating COVID-19, there are always potential side effects and adverse effects that are associated with these synthetic drugs. Thus, herbs that possess potent antiviral activities serve as alternatives to synthetic drugs to inhibit viral replication. [13] Various traditional medicines were used to prepare herbal formulations to treat COVID-19 and its complications effectively.[14][15][16][17] Also, investigations were conducted to prove the antiviral, especially against anti-COVID-19 activity possesses potent thrombolytic activity of herbs.[18] One of the herbs of interest that possess both antiviral and thrombolytic activity as per Traditional Indian Siddha text is Bambusa bambos.

The leaf, shoot, node, root, and seeds of the plant are mainly used in Siddha medicine. According to Kuṇapāṭam- poruṭpaṇpu nūl MooligaiVaguppu written by Murugesa Mudaliyar the whole plant possesses Veppamuṇṭākki (Stimulant), Tuvarppi (Astringent), Uramākki (Tonic), Icivakaṟṟi (Antispasmodic), Kāmamperukki (Aphrodisiac) and especially the leaves possess Ruvuṇṭākki (Emmenagogue), Puḻukkolli (Anthelimintic) actions.

"Kuṭaṟkaṭṭuccūlaiyuṭaṉkuṉmam

utiramuṭaṟkeṭṭātōṭiyoḻiyum - aṭaṟṟaṅku

vēlviḻimātēkēḷāy! Vēyiṉilaitaṉakkuk

kālvaḻiyuñcōṇitam, pōṅkāṇ."

According to the above verse in Tēraiyar kuṇavākaṭam the leaves of the plant cure Kuṭaṟcūlai (intestinal colic), Vayiṟṟunōvu (gastric pain), Kurutittaṭippu (thrombosis) and Cūlakaaḻukku (lochia). Siddha compound medicine cūtakuṭaippukuṭiṇīrcūraṇam (cikiccāraṭṉatīpam), caturmukakuḷikai (cukātārakaḷañciyam) and adjuvant in veḷvaṅkacentūram (Siddha Materia medica – Mineral Kingdom) are few siddha preparations prepared from Bambusa bambos leaves to cure amenorrhoea, oligomenorrhoea, stroke, and malignant intestinal tumours.

Thus, the present study was conducted to prove the thrombolytic activity and anti-coagulant activity of extracts of Bamboo plant leaves using in vitro studies and in-silico experiments. This study also aims to identify essential components in bamboo leaves and develop novel de novo medicine for COVID-19 Vaccination Associated Coagulopathy from Bambusa bambos leaves using an artificial intelligence-assisted WADDAICA tool. This attempt also aims to standardize the plant, Bambusa bambos using advanced scientific techniques.

2. Materials and Methods

2.1 Collection and Authentication

The plant was collected in Alanganalore, Madurai District, India and authentication was done by Dr. Sunil, Department of Pharmacognosy, Siddha Central Research Institute, CCRS, Chennai, India.

2.2 Microscopic examination

The leaf sample was preserved in fixative formalin for more than 48 h. The preserved specimens were cut into thin transverse sections using a rotary microtome and the sections were stained with various stains to highlight different parts of the tissue.[19] Transverse sections were photographed using an Axiolab 5 trinocular microscope attached with a Zeiss Axiocam 208 color digital camera under bright field light.

2.3 Powder Microscopy

A small amount of the powdered sample was mounted on a microscopic slide with a drop of 50% glycerol after clearing with a saturated solution of chloral hydrate.[20] Characters were observed using a Nikon ECLIPSE E200 trinocular microscope attached to a Zeiss ERc5s digital camera under field light.

2.4 Scanning Electron Microscopy (SEM)

SEM images of the powdered plant leaves were analyzed at various magnifications to examine the topography of the powdered plant material.

2.5 Determination of Particle Size Variations

The determination of the mean of the particle size of the powder particles was performed using PCS in conjugation with Zetasizer Nano ZS-90 (Malvern Instruments Ltd., UK). The readings were carried out at an angle of 90^0 to the incident radiation. The Zeta potential was measured by a laser Doppler anemometer attached to the above instrument at ±150mV as the initial potential.[21]

2.6 DNA Barcoding

100 mg of plant powder in a centrifuge tube was incubated with 1 ml of preheated CTAB extraction buffer containing 20 µl of β-mercaptoethanol 65°C for 30min and centrifuged for 10min at 12000 rpm. The supernatant was collected and chloroform: isoamyl alcohol (1:1) was added and an emulsion was formed. This was centrifuged at 13000 rpm for 12 min and the clear aqueous phase was collected. It was mixed with ice-cold isopropanol incubated overnight at -20°C and centrifuged at 12, 000 rpm for 3 min. The pellet was washed with 70% ethanol, air-dried, and suspended in T10E1 buffer (20-30 µL). Qualitative and quantitative assessment of the DNA included running samples on 1% agarose gel for band visualization under UV light and quantification using Nanodrop. PCR amplification using the rbcL DNA barcode was confirmed by gel electrophoresis. Sequence analysis involved obtaining FASTA-formatted nucleotides from chromatograms using Finch TV, followed by BLAST analysis on NCBI to identify species matches in GenBank. Finally, sequences were submitted to NCBI for GenBank ID acquisition and converted to barcodes using BioRad software.

2.7 Extraction of leaves of Bamboo

The powdered leaves of Bambusa bambos (50 g) were extracted with methanol using a soxhlet apparatus. The extract was collected and filtered using filter paper. The filtrates were reduced using a rotary evaporator and the solid mass of each extract (BLE-29.44%%w/w) was collected and stored in airtight containers at 4°C till use. [22]

2.8 Preliminary Phytochemical Screening

The dry extract was tested for various chemical constituents like carbohydrates, proteins, glycosides, alkaloids, phenols, steroids, flavonoids, tannins, volatile oils, fats, saponins, etc. [23]

2.9 Quantitative Study of Phytochemicals

2.9.1 Total Phenol Content (TPC)

The total Phenol content of the extract was determined using standard procedure.[24] 1ml of extract (100 µg/mL) was added to Folin Ciocalteu reagent (2.5ml; 10% w/v). This solution was mixed with Sodium carbonate solution (2 ml; 75%) and allowed to settle for 5min. The solution was allowed to react for 10 min at 50°C with continuous stirring and was subjected to UV to measure absorbance at 765 nm. The standard curve of Gallic acid was constructed with various concentrations (50, 100, 150, 200, and 250 µg/mL) using a similar method, and the TPC of the extract was counted as mg of gallic acid equivalents (GAE)/g of dry extract.

2.9.2 Total Flavonoid Content (TFC)

The flavonoid content of the methanol extract was determined using Dowd's method.[25] The standard drug (Quercetin) was dissolved in distilled water (25, 50, 100, 150, and 200 µg/mL) and mixed with aluminum chloride solution (2ml;10%w/v) with methanol and potassium acetate solution (0.2 ml;1 M). The reaction mixture was incubated at 35°C for 30-45 min and subjected to measurement of absorbance at 415 nm. The standard curve of quercetin was drawn and the whole procedure was performed using methanol extract (100 µg/mL) to measure TFC in quercetin equivalents (QE) expressed as mg QE/g of dry extract.

2.9.3 Total Condensed Tannin Content (TTC)

To 50µl of methanol extract (10% w/v), vanillin solution (3ml of 4%w/v in methanol) was added and finally mixed with 1.5 ml of conc. HCl. This reaction medium was left to react for 15 min and absorbance was estimated at 500 nm against methanol. The TTC was expressed as mg of catechin equivalents (CE) per gram (mg CE/g) of extract.[26]

2.10 HPTLC Fingerprinting Profile

A 5 µL of standard quercetin solution (S1) (1 mg/mL in methanol) and 5, 10 µL of test solutions (T1, T2) (1 mg/mL of methanol extract in methanol) were spotted on a precoated silica gel 60 F_{254} HPTLC plate (E. Merck) of uniform thickness 0.2 mm using Linomat 5 sample applicator on the stationary phase, Silica Gel 60 F_{254}. The plate was developed in the solvent system (Toluene: Ethyl acetate: Formic acid (5:4:1)) to a distance of 8 cm. The bands were observed under UV light at 254 nm using CAMAG REPROSTAR3.[27]

2.11 GCMS study

The GC-MS study of the methanol extract of B. bambos was performed using the Thermo-GC-Trace Ultra (5) and Thermo-MS-DSQ (II) equipment. The analysis utilized a non-polar DB (35) MS column with Capillary Standard, measuring 30mmx0.25mmx0.25µm film. A flow rate of helium was set at 1 mL/min. The determination of constituents was dependent on compound libraries by Willey and NIST, incorporating retention indices integrated into the GC-MS instrument for comparison.[28] [29]

2.12 In vitro Studies

2.12.1 Antimicrobial Activity

The antimicrobial activity was assessed using the Kirby-Bauer disc diffusion method. Mueller-Hilton Agar plates were infected with 100 µl cultures of Serratia marcescens (MTCC 86), Bacillus subtilis (MTCC 1133), Pseudomonas aeruginosa (MTCC 3541), Enterococcus faecalis (MTCC 439), Staphylococcus aureus (MTCC 96), and Escherichia coli (MTCC 452). Similarly, Sabouraud Dextrose Agar plates were inoculated with 100 µl cultures of Candida albicans (MTCC 854) and Aspergillus niger (MTCC 281). Discs with varied quantities of extract (BLE-162.5, 325, 750, 1500, and 3000 µg/10µL), vehicle control (DMSO), and positive controls (10 µg/10µL) (Ciprofloxacin for bacteria, Amphotericin B for fungi) were placed on the appropriate plates. To assess the antibacterial activity of the extracts, all bacterial plates were incubated at 37°C for 24 h, while A. niger plates were incubated at 37°C for 48 h.[22] [30]

2.12.2 Antioxidant Assay using DPPH Assay

5µl of various concentrations of Ascorbic acid (0.78-50 µg/mL) and BLE (1-1000 µg/mL) was added to 0.1 mL of 0.1mM DPPH solution in a 96 well plate. The plate was incubated for 30 min in the dark and the absorbance was measured at 517nm using a microplate reader (iMark, BioRad) against the blank solution (0.2 mL DMSO/Methanol). A reaction mixture containing 20µl of deionized water without drug was served as Control. [31][32][33]

The percent inhibition was calculated using the formula:

$$\% \text{ inhibition} = ((Abs_{Control} - Abs_{Sample})/Abs_{Control}) \times 100$$

2.12.3 In vitro activity in cell lines

The HaCaT cells (procured from NCCS Pune) were cultured in 96 well plates (10^4 cells/well) for 24 h in DMEM medium (Dulbecco's Modified Eagle Medium-AT149-1L) supplemented with 10% FBS (Fetal Bovine Serum-HIMEDIA-RM 10432) and 1% antibiotic solution (Penicillin-Streptomycin-Sigma-Aldrich P0781) at 37°C with 5% CO_2.

2.12.4 In vitro Cytotoxicity of BLE on HaCaT Cell lines

The cells were incubated overnight on the DMEM medium in a 96-well plate and were exposed to 100 µL of various concentrations of BLE (1-1000 µg/mL) dissolved in the DMEM medium. The cells were incubated for 12 h and washed using Phosphate buffered saline (PBS) twice. 20 µL MTT along with 5 mg/mL PBS was added to each well, followed by incubation at 37°C in 5% CO2 for 2–4 h. The resultant cells were washed with excess PBS and mixed with 150µL DMSO per well with shaking for 10 min at 120rpm. Absorbance was measured at 570nm using

a Microplate Reader using untreated cells as control.[34][35] Cell proliferation was calculated as per the following formula

$$\%\text{Cell viability} = (A_{test}/ A_{Control}) *100$$

A_{test} = Absorbance of test sample; $A_{Control}$ = Absorbance of Control

2.12.5 In vitro wound healing activity using HaCaT cell lines

The cells were incubated on the culture plate for 24 h and after ensuring complete growth the plate was scratched using the tip of the micro pipette. The cells were treated with 100µL of extract dissolved in the culture medium (50 µg/mL) and allowed to incubate for 24 h.[36] The culture medium was photographed and the area of the scratch was analyzed using Image J Software (NCBI) and further presented in graphical format. Images were captured under an inverted microscope (Olympus ek2) using a Camera (AmSope digital camera 10MP Aptima CMOS). The cells that did not receive any drug treatment were considered as controls.

2.12.6 In vitro Anticoagulant Activity

Determination of clotting time and prothrombin time

Fresh chicken blood (10 mL) was collected from a local butcher shop. 5 mL of the blood was used for clotting time measurement and the rest was mixed with 5 mL of calcium chloride solution (1g/mL distilled water), centrifuged at 3000rpm for 15min, and the supernatant plasma stored at -4°C. In clotting tubes, 0.5 mL of PBS, BLE-P (5, 10, 15, and 20 mg/mL in PBS), and acid citrate dextrose were transferred and incubated for 10 min at 37ºC. The tubes were slanted at 45º to check the clot formation. The time taken for the observation of the first clot was noted and slanting of tubes was continued further till the flow of the blood was stopped. The time taken for complete clotting of the blood was noted as clotting time and % activity was determined. The stored plasma (0.2 mL) was poured into coagulation tubes with one tube considered as normal control. 0.1 mL of PBS and BLE-P were added to the plasma and swiftly shaken and allowed to settle and the time was noted. The tubes were gently tilted at 45ºc until permanent clots were observed. This was considered as prothrombin time.[37][38]

The following formula was used to determine the % activity.

$$\%\text{ activity} = (Tc/Tt) \times 100$$

Where, Tc=Time of a clot of the control group; Tt=Time of a clot of test

2.12.7 In vitro Thrombolytic Activity Test

The weight of the clot after calculating the clotting time is noted after the separation of plasma. 100µl of BLE solution of various concentrations (5, 10, 15, and 20 mg/mL in PBS) was separately added to the centrifuge tubes. The tubes were incubated at 37°C for 90 min without any disturbance and clot lysis was observed. After incubation, fluid released was carefully removed and tubes were again weighed to observe the difference in weight after clot disruption.[39] [40] The % thrombolysis was calculated from the following formula

$$\%\text{Clot lysis} = 100 - \frac{\text{Wcf}}{\text{Wc}}\text{x}100$$

Where, Wcf=Weight of clot after lysis; Wc=Weight of clot

2.13 Molecular Docking of Phytocompounds in Bambusa Bambos

The structures of 16 potentially active compounds of Bambusa bambos identified from the GC-MS analysis were retrieved from the IMPPAT (Indian Medicinal Plants, Phytochemistry and Therapeutics) server in .pdb format and slightly modified for molecular docking analysis using MGL AutoDock Tools 1.5.7. Structural data of the standard drugs, Rivaroxaban, Dabigatran, Clopidogrel, and Warfarin were extracted from the PubChem database and were used for the comparative study as a positive control. The Vitamin-K epoxide reductase (PDB ID: 3KP9) Antithrombin III (PDB ID: 2B4X) Thrombin (PDB ID: 1KTS) and Factor X (PDB ID: 1KSN) were also downloaded in .pdb format. Removal of water molecules along with the addition of hydrogen bonds and Kollman charges were performed. Computational docking was performed to achieve a group of permissible orientations and conformations for the ligand at the binding site. The native ligand position was determined on the binding site by arranging the grid coordinates (X, Y, and Z). The docking studies were carried out using the Lamarckian genetic algorithm. The following docking parameters were chosen for AutoDock4 runs: 10 docking runs, 150 population size, 0.02% mutation rate, and 0.8 crossover rate. The grid parameter file (gpf) was created with AutoGrid 4.0, while the dock parameter file (dpf) was created with AutoDock 4.0. The Discovery Studio Visualizer program was used in the analysis of 2D and 3D Hydrogen-bond interactions of the complex receptor-ligand structure and to identify the interactions of the receptor with the ligand.

2.14 Molecular Docking for De Novo Drug

In this study, 5 de novo drugs have been designed using WADDAICA webserver with the underlying chosen phytocompounds and docked with target proteins such as Factor X (PDB ID: 1KSN), Thrombin (PDB ID: 1KTS), Antithrombin III (PDB ID: 2B4X) and Vitamin-K epoxide reductase (PDB ID: 3KP9). De novo drug model 1 comprised of alpha-cubebene, de novo drug model 2 comprises of diethyl phthalate, de novo drug model 3 comprises of diisooctyl phthalate, de novo drug model 4 comprises of 3, 7, 11, 15-Tetramethyl-2-hexadecen-1-ol and de novo drug model 5 comprises of (24E)-24-N-Propylidenecholesterol. Each model has been evaluated based on several drug-likeness criteria such as Lipinski, Ghose, Veber, and Egan rules, along with a bioavailability score of 0.55, indicating their potential as drug candidates.

3. Results

3.1 Physicochemical parameters of leaf powder

The physicochemical evaluation of the Bambusa bambos powder was performed and the results are under acceptable limits as per pharmacopoeia as shown in Table 1.

Table 1: Physicochemical parameters of the leaf powder

S No	Parameters	Results
1	Description	Green-coloured fine powder
2	pH (1%w/v solution)	5.90
3	Total ash	12.26 %w/w
4	Acid insoluble ash	10.01 %w/w
5	Loss on drying at 105°C	1.70 %w/w
6	Water Soluble Extractive (WSE)	14.2 %w/w
7	Alcohol Soluble Extractive (ASE)	5.75 %w/w
8	Bulk density	0.2783 g/mL
9	Tapped density	0.4373 g/mL

3.2 Microscopic Examination

The transverse section (TS) of the leaf sample shows a slightly sinuous upper and lower epidermis covered with a thick cuticle and numerous cuticular outgrowths in the lower epidermis. Both epidermis layers contain enlarged rectangular bulliform cells with silica deposits and inward-curved walls, arranged in 3-4 cell lines extending into the mesophyll. The mesophyll consists of closely packed plicate cells, resembling palisade parenchyma, and colorless horizontally arranged fusoid cells. The plicate cells form 2-3 layers, while the translucent polygonal fusoid cells form a single layer. In the midrib region, a single vascular bundle is present towards the lower epidermis, and two smaller bundles are towards the upper epidermis, all capped with well-defined sclerenchymatous bundle sheaths. These bundles are conjoint, collateral, closed, and composed of normal vascular elements. In the lamina region, small vascular bundles, capped by sclerenchymatous sheaths, are adjacent to the fusoid cells and extend towards both epidermis layers as shown in Fig.1-3.

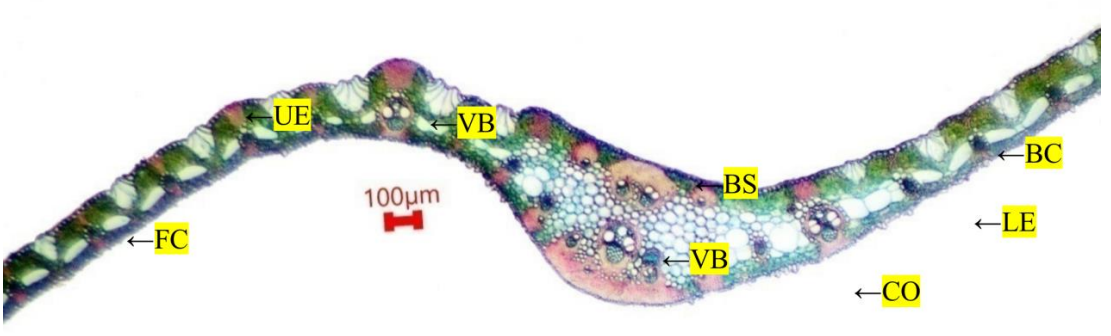

Fig 1: Transverse section of the leaf of Bambusa bambos

BC – bulliform cell; BS – bundle sheath cell; CO – cuticular outgrowth; Cu – cuticle; FC – fusoid cell; LE – lower epidermis; Pa – parenchyma; PC – plicate cell; PF – phloem fibre; Ph – phloem; UE – upper epidermis; V – vessel; VB – vascular bundle; Xy – xylem

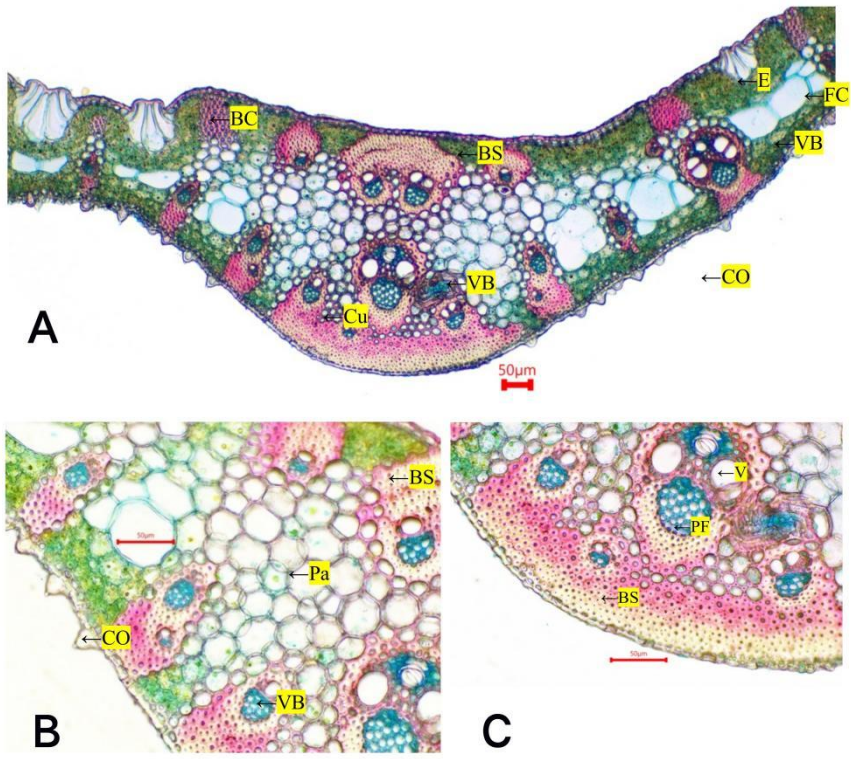

Fig 2: Transverse section of the midrib section of the leaf of Bambusa bambos

A.Midrib region; B.Lateral region of midrib enlarged; C. Lower region of midrib enlarged

BC – bulliform cell; BS – bundle sheath cell; CO – cuticular outgrowth; Cu – cuticle; FC – fusoid cell; LE – lower epidermis; Pa – parenchyma; PC – plicate cell; PF – phloem fibre; Ph – phloem; UE – upper epidermis; V – vessel; VB – vascular bundle; Xy – xylem

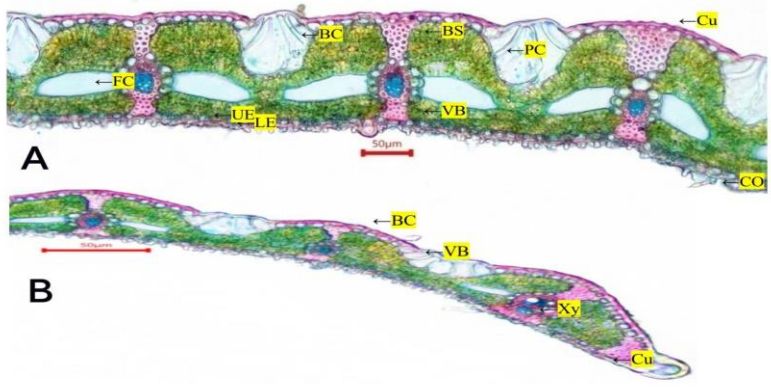

Fig 3: Transverse section of the Lamina of the leaf of Bambusa bambos

A.Lamina region; B.Lamina margin enlarged

BC – bulliform cell; BS – bundle sheath cell; CO – cuticular outgrowth; Cu – cuticle; FC – fusoid cell; LE – lower epidermis; Pa – parenchyma; PC – plicate cell; PF – phloem fibre; Ph – phloem; UE – upper epidermis; V – vessel; VB – vascular bundle; Xy – xylem

3.3 Powder microscopy

The powder, which is chaff green in color with no characteristic odor or taste, showed the presence of epidermis with numerous outgrowths, plicate cells, reticulate and pitted vessels, and thick-walled fibres with a narrow lumen.

3.4 Histochemical observations

The histochemical tests showed the presence of cutin on the cells of the upper and lower epidermis (Fig. 4); alkaloids were present in a few epidermal cells and the plicate cells, lignin deposition was observed along the walls of xylem elements and surrounding the vascular bundles and mucilage was absent.

Fig: 4 Powder microscopy Bambusa leaf

A. Phenol and alkaloid compound; B. Cutin; C. Lignin

3.5 Particle Size Analysis (SEM and Zeta)

The SEM images of the leaf powder suggested the presence of small irregular particles placed over smooth planes. These particles had a nano formation and rodlike structure. SEM image

magnification at 1kx, 2 kx, 5 kx, 10 kx, 15 kx, 30 kx, 50 kx, 70kx 200 kx, and 500 kx are measured as in fig.5. WD ranged between 5.08mm and 5.11mm. High voltage power supplies for SEM are 10.0Kv. The zeta potential report also shows good stability of the particles in the powder which contributes to aggregation with a potential of -17.9mv. (Fig 5)

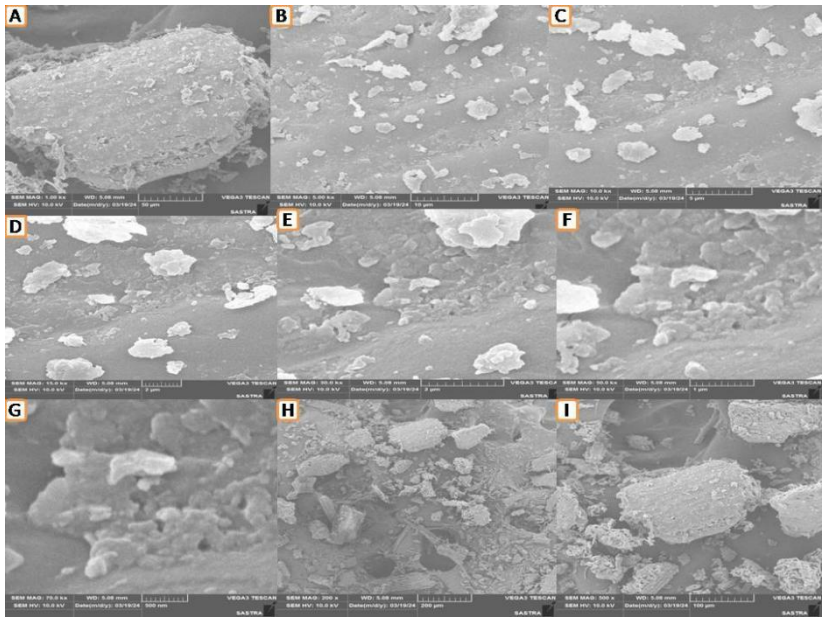

Fig 5: SEM Images of leaf powder of B.bambos

A.1kx; B.5kx; C.10kx; D.15kx; E.30kx; F.50kx; G.70kx; H.200kx; I.500kx

Results

		Mean (mV)	Area (%)	St Dev (mV)
Zeta Potential (mV):	-17.9	**Peak 1:** -17.9	100.0	6.84
Zeta Deviation (mV):	6.65	**Peak 2:** 0.00	0.0	0.00
Conductivity (mS/cm):	0.162	**Peak 3:** 0.00	0.0	0.00
Result quality :	Good			

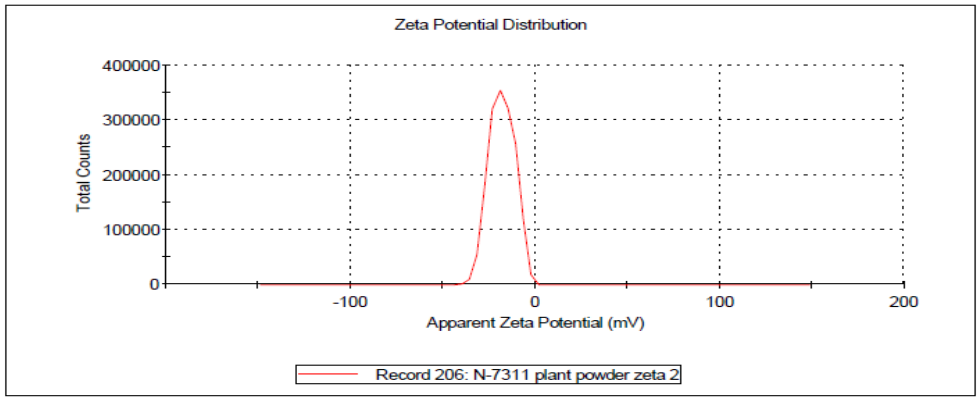

Fig 6: Zeta Potential Report of B.bambos leaf powder

3.6 DNA Barcoding

The genomic DNA was isolated from the authenticated Bambusa spp. The sample exhibited a concentration of 636.50ng/µL with an A_{260}/A_{280} and A_{230}/A_{260} ratio of 2.15 and 1.32 respectively, indicating minimal contamination by proteins and polysaccharides. Gel electrophoresis of the PCR amplified sample, alongside a 100 bp DNA ladder, confirmed successful amplification (Fig. 7). Sequential analysis using ITSPF5 marker revealed a specific genetic sequence, subsequently converted into a barcode format and submitted to GenBank for identification.

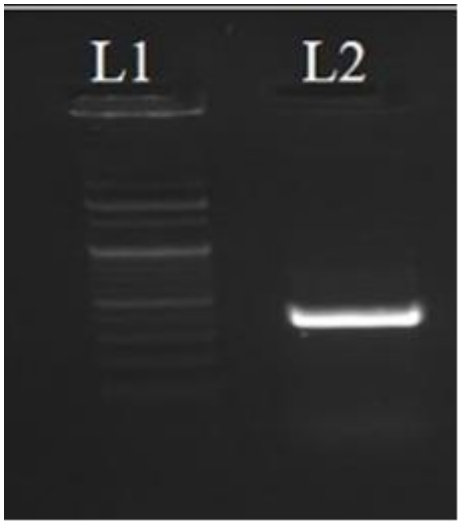

Fig 7: Gel image of PCR amplified sample

L1: DNA ladder; L2: Bambusa

3.7 Preliminary phytochemical screening

The results of the phytochemical screening of the methanol extract of Bambusa bambos powder indicated the presence of Carbohydrates, flavonoids, proteins, sterols, and tannins.

3.8 Quantitative study of phytoconstituents

The methanol extract of Bambusa bambos contained 7.215% total flavonoids, 7.421% total phenols, and 0.3668% total condensed tannins as shown in Table 2.

Table 2: Phytocompounds in the methanol extract of Bambusa bambos

Compound	Quantity %
Total Flavonoid Content	7.215
Total Phenol Content	7.421
Total Condensed Tannin Content	0.3668

3.9 HPTLC Fingerprinting

HPTLC fingerprinting analysis as shown in Table 3 and Figs. 8 and 9 revealed R_f-0.61 corresponding to Quercetin (S1) and for samples T1 and T2 various peaks at different Rf values were recorded out of which peak 5 in sample T1 corresponded to the standard,

Quercetin.

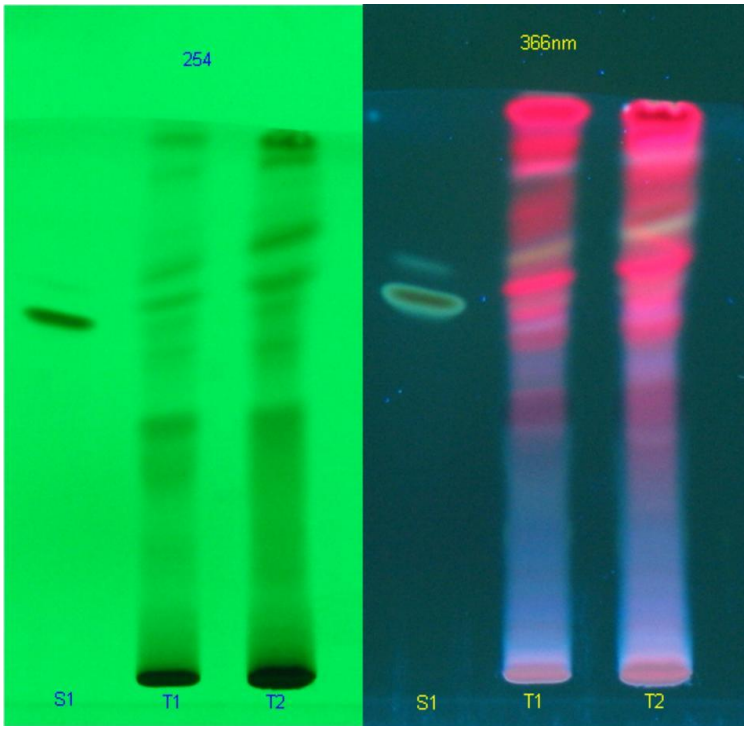

Fig 8: HPTLC analysis of the methanol extract of leaves of B.bambos

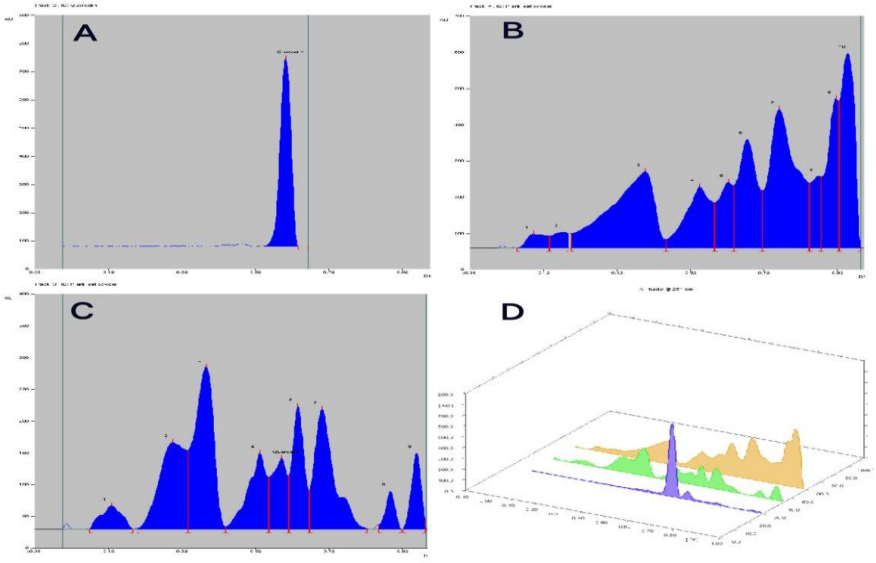

Fig 9: HPTLC chromatograms of A. Quercetin (S1); B. test sample (T1); C. test sample (T2); D. Overlay spectra

Table 3: Rf values of the respective peaks in chromatograms

Peak	Rf value	Height	Area	Area %
Quercetin (S1)				
1	0.61	666.7	14867.3	100.00
T1-Test sample				
1	0.13	36.6	1578.7	3.70
2	0.30	136.7	7402.4	17.34
3	0.39	255.4	10004.2	23.43
4	0.54	119.7	4437.7	10.40
5	0.60	111.3	3334.3	7.81
6	0.64	193.2	4772.7	11.18
7	0.71	188.9	7610.1	17.83
8	0.89	60.1	1160.8	2.72
9	0.96	119.6	2388.3	5.99
T2-Test sample				
1	0.10	38.2	1539.1	1.57
2	0.18	44.4	1402.4	1.43
3	0.40	210.8	19014.3	19.42
4	0.55	169.2	8766.4	8.95
5	0.63	181.1	5540.8	5.66
6	0.68	300.1	11410.9	11.65
7	0.77	382.9	21462.6	21.92
8	0.87	198.1	3992.7	4.08
9	0.92	411.6	9848.2	10.06
10	0.95	537.6	14946.6	15.26

3.10 GC-MS profile of Bambusa bambos

The GC-MS analysis of the methanol extract of leaves of Bambusa bambos revealed the presence of 33 compounds which are tabulated in Table 4 and the chromatograms were depicted in Fig. 10. Chromatogram identified Diisooctyl phthalate, 3, 7, 11, 15-Tetramethyl-2-hexadecen-1-ol, alpha-Cubebene, and Dibutyl phthalate as major chemical constituents alongside Squalene, Pentadecanoic acid, Neophytadiene, Benzyl Benzoate and 2-methyl-Octacosane.(Fig 10)

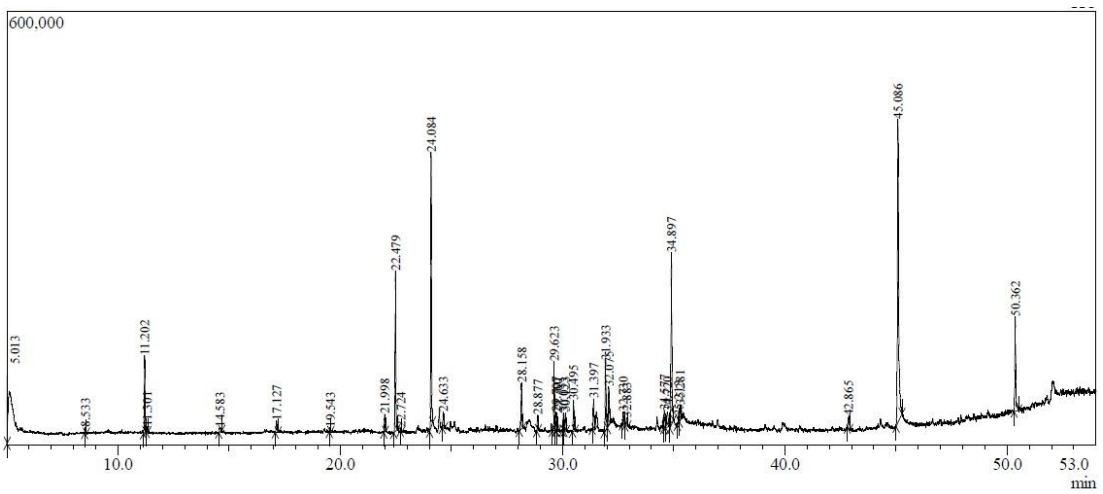

Fig 10: GC-MS Chromatogram of Bambusa bambos

Table 4: GC-MS analysis of methanol extract of leaves of Bambusa bambos

Peak#	R.Time	Area	Area%	Similarity	Name
1	5.013	50186	0.76	91	N-methyl-2-amino-Propanamide
2	8.533	22008	0.33	84	1, 1-dimethoxy-Cyclohexane
3	11.202	231868	3.52	86	2-methyl-Octacosane
4	11.301	15564	0.24	80	Decanal
5	14.583	24364	0.37	85	4-Vinylphenol
6	17.127	58514	0.89	87	2-Methoxy-4-vinylphenol
7	19.543	12404	0.19	72	2, 6, 11-trimethyl-Dodecane
8	21.998	63240	0.96	83	(1S, 4aR, 8aS)-1-Isopropyl-7-methyl-4-methylene-1, 2, 3, 4, 4a, 5, 6, 8a-octahydronaphthalene
9	22.479	572464	8.68	88	alpha-Cubebene
10	22.724	11488	0.17	73	5, 6, 7, 7a-tetrahydro-4, 4, 7a-trimethyl-, ®-2 (4H)-Benzofuranone
11	24.084	959898	14.56	96	Diethyl Phthalate
12	24.633	58087	0.88	85	(1R, 9R, E)-4, 11, 11-Trimethyl-8-methylenebicyclo[7.2.0]undec-4-ene
13	28.158	198973	3.02	94	Benzyl Benzoate
14	28.877	53005	0.80	92	Heptadecane
15	29.623	240141	3.64	95	Neophytadiene
16	29.707	62556	0.95	82	6, 10, 14-trimethyl-2-Pentadecanone
17	29.760	66196	1.00	84	3, 7, 11, 15-Tetramethylhexadec-2-ene
18	30.033	60485	0.92	87	bis (2-methylpropyl) ester 1, 2-Benzenedicarboxylic acid
19	30.123	72754	1.10	86	3, 7, 11, 15-Tetramethylhexadec-2-en-1-yl acetate
20	30.495	109932	1.67	91	3, 7, 11, 15-Tetramethyl-2-hexadecen-1-ol
21	31.397	115375	1.75	95	methyl ester Hexadecanoic acid
22	31.933	279804	4.24	96	Dibutyl phthalate
23	32.075	172975	2.62	90	Pentadecanoic acid
24	32.730	58632	0.89	80	Ethyl tridecanoate
25	32.883	38794	0.59	81	2-Methyltetracosane
26	34.577	62637	0.95	81	propyl ester trans-9, 12-Octadecadienoic acid

27	34.720	90777	1.38	78	methyl ester, (Z)-6-Octadecenoic acid
28	34.897	658306	9.99	94	3, 7, 11, 15-Tetramethyl-2-hexadecen-1-ol
29	35.213	23368	0.35	65	Methyl stearate
30	35.281	56513	0.86	81	11, 14-Eicosadienoic acid
31	42.865	53382	0.81	86	1, 3, 5-triphenyl-Cyclohexane
32	45.086	1640954	24.89	90	Diisooctyl phthalate
33	50.362	397098	6.02	93	Squalene
		6592742	100.00		

3.11 Antimicrobial Activity: Zone of Inhibition

The methanol extract of Bambusa bambos extract exhibited antimicrobial activity against all tested organisms. The zones of inhibition were measured and compared to positive controls, demonstrating significant inhibitory effects, particularly against P. aeruginosa and A. niger.

Table 5: Antimicrobial activity of methanol extract of Bambusa bambos

Slno	Organism	Concentration of BLE (µg/mL)	Zone of inhibition (mm)		
			BLE	Amphotericin B (50 µg/mL)	Ciprofloxacin (10 µg/mL)
1	S. marcescens	750	9.33	--	31.66
2	B. subtilis	3000	9.66	--	31
3	P. aeruginosa	3000	10	--	25
4	E. faecalis	1000	9	--	24.66
5	S. aureus	3000	9	--	26.33
6	E. coli	750	8.5	--	29.5
7	C. albicans	750	8	21.333	--
8	A. niger	3000	13.33	23	--

3.12 In vitro Anti-oxidant Assay in DPPH assay

The in vitro antioxidant activity of the methanol extract of Bambusa bambos was investigated using the DPPH method. The extract showed similar activity in comparison to the standard drug, Ascorbic acid. The IC_{50} values of Ascorbic acid and BLE were calculated as 8.95 and 59.6 µg/mL respectively which denoted that the extract possessed antioxidant activity as shown in Fig. 11.

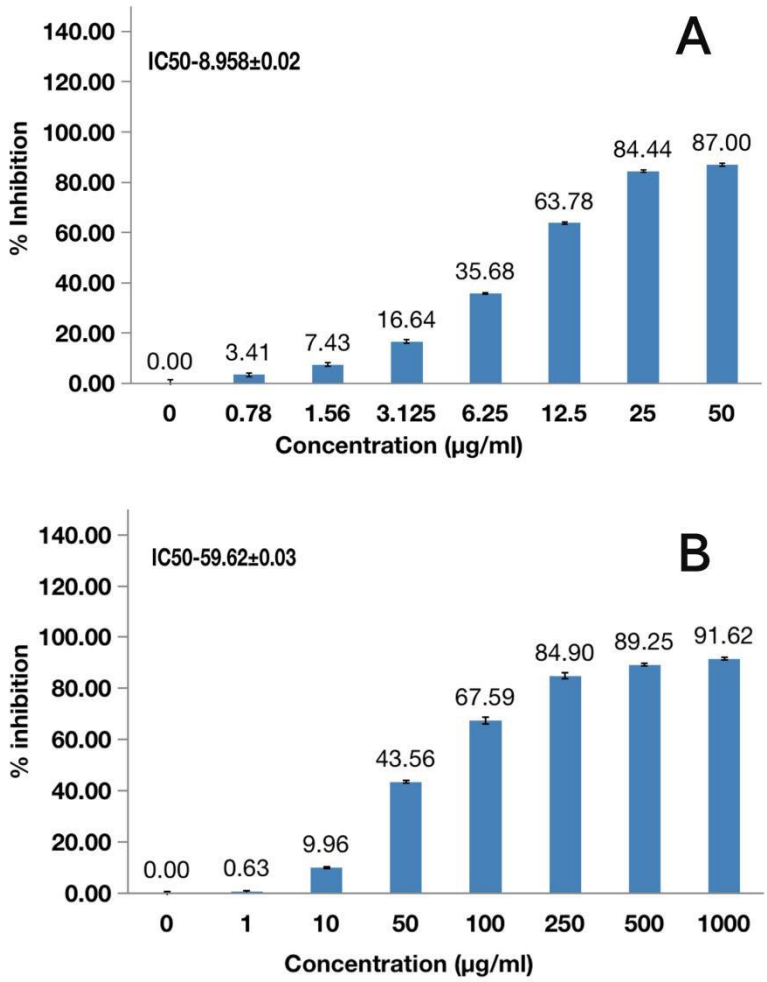

Fig 11: Antioxidant activity of methanol extract of Bambusa

A. Ascorbic acid; B. BLE

3.13 In vitro Cytotoxicity of Bambusa bambos on HaCaT cell lines

Based on the results obtained from the MTT assay, it was observed that when the HaCaT cell line was exposed to different concentrations of methanol extract of Bambusa (BLE) ranging from 1-1000 µg/mL, IC_{50} value was determined as 64.35 µg/mL and the respective % viability towards each concentration were shown in figure 12. The cell morphology study in Fig. 13 revealed that the extract induced cytotoxicity at 250 µg/mL which showed marked condensation of the nucleii and aggregation of cells.

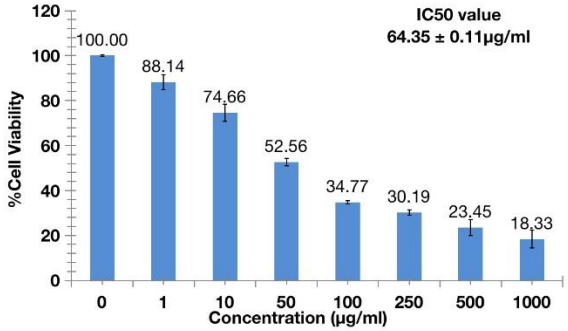

Fig 12: The graph has a Y-axis representing % of viable cells and X-axis shows the levels of concentration

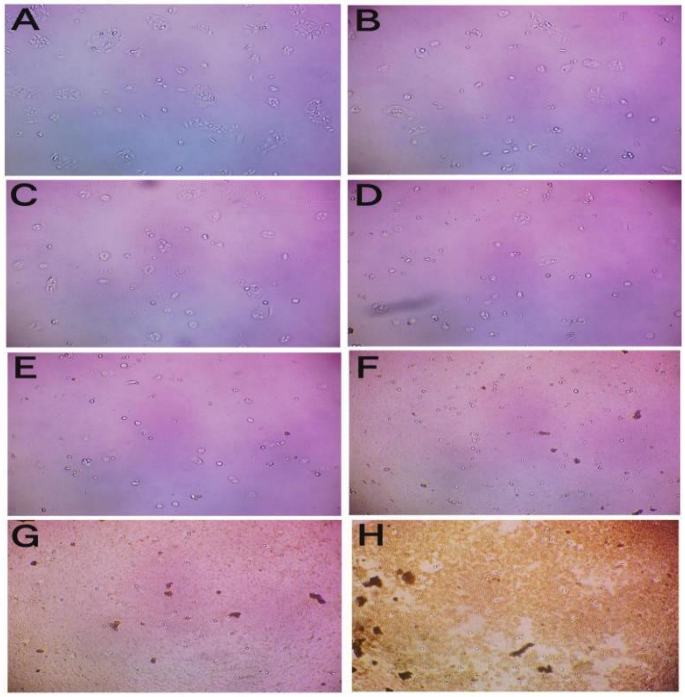

Fig 13: Cell morphology of HaCaT cell lines treated

A. control; B. BLE-1 µg/mL; C. BLE-10 µg/mL; D. BLE-50 µg/mL; E. BLE-100 µg/mL; F. BLE-250 µg/mL; G. BLE-500 µg/mL; H. BLE-1000 µg/mL

3.14 In vitro Scratch Assay in Cell line- HaCaT

Based on the results obtained from the scratch assay, HaCaT cells were treated with different doses of BLE which healed the scratched area better than the control group after 24 h. A positive result was observed in treated and Control (Cells without treatment) i.e. gap was healed up to 26.01% while in treated cells with sample-1, at 50 µg/mL (33.67%) as shown in fig 14.

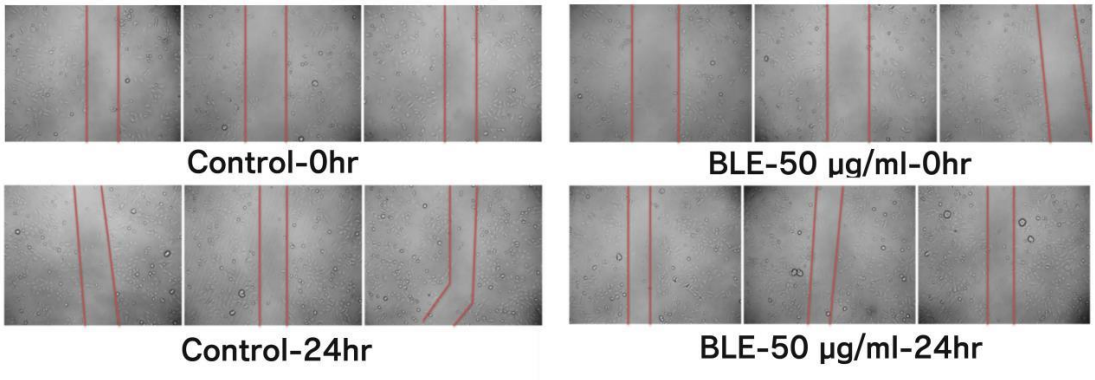

Fig 14: In vitro wound healing activity of methanol extract of Bambusa bambos on HaCaT Cell lines

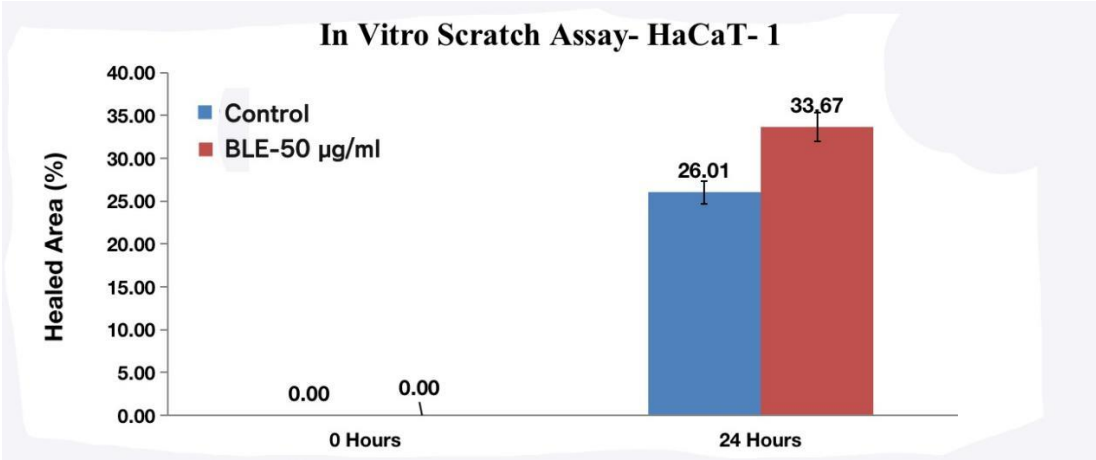

Fig 15: Represents the graph and picture showing % of the unhealed area and healed area

Table 6: Wound healing activity of methanol extract of Bambusa bambos on HaCaT Cell lines

Group	% healing	
	0hr	24hr
Control	0±0	26.01±2.43
BLE-50 µg/mL	0±0	33.67±4.47***

The values were expressed as Mean±SEM (n=3)

3.15 In vitro Anticoagulant Activity

The in vitro anticoagulation activity was investigated using chicken blood and the results revealed that the methanol extract of Bambusa bambos exhibited dose-dependent anticoagulant activity with 261% activity at 20 mg/mL compared to the control group. On the other hand, % prothrombin inhibition also significantly increased by the treatment with BLE at 20 mg/mL in a dose-dependent manner. The clotting time was significantly increased from 315.33 sec in the control group to 824.66 sec in the BLE 20 mg/mL group as shown in Table

7. Prothrombin time also was significantly and dose dependably increased with the treatment of BLE in comparison to the control.

Table 7: Effect of methanol extract of Bambusa bambos leaves (BLE) on clotting time

Conc	Clotting Time (sec)	% anti-coagulant activity	Prothrombin Time (PT)	% prothrombin Inhibition activity
Control	315.33±20.402	100±6.470	22.33±2.516	100±11.27
BLE (5 mg/mL)	441.33±27.682	139.95±8.778	60.66±2.516	271.68±11.27
BLE (10 mg/mL)	558.66±26.501	177.16±8.404	86.33±3.785	386.62±16.954
BLE (15 mg/mL)	659.33±33.560	209.09±10.643	125.33±4.041	561.27±18.098
BLE (20 mg/mL)	824.66±23.713	261.52±7.520	167.66±4.725	750.85±21.263

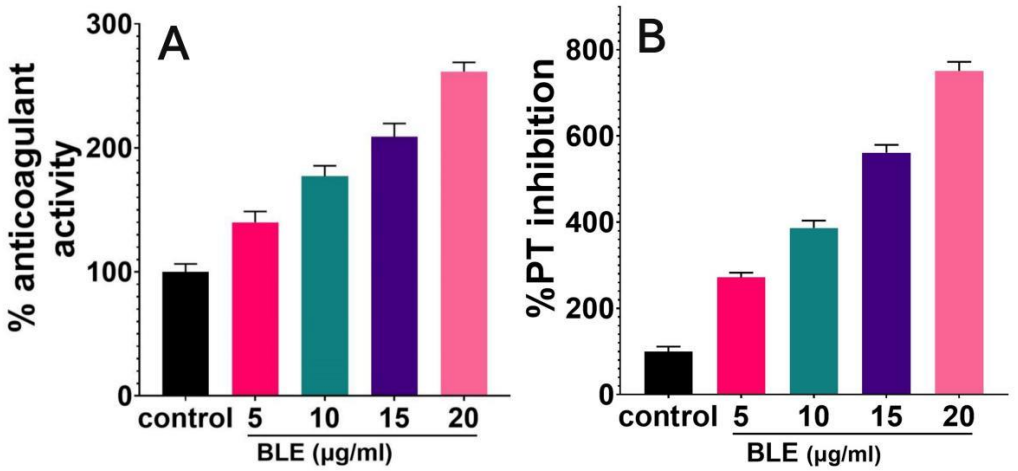

Fig 16: Anticoagulant activity of BLE

3.16 In vitro Thrombolytic Activity

The methanol extract of Bambusa bambos (BLE) exhibited significant thrombolytic activity compared to the control group in the chicken blood. The results were tabulated in Table 8 which suggests that BLE showed dose-dependent activity. The extract showed maximum activity of 68% at 20 mg/mL.

Table 8: Thrombolytic activity of methanol extract of Bambusa bambos leaves

Concentration	Weight of clot before lysis (g)	Weight of clot after lysis (g)	%thrombolysis
Control	0.2773±0.0185	0.2690±0.0159	2.952±1.693
BLE (5 mg/mL)	0.2865±0.0183	0.2486±0.0128**	13.133±2.015**
BLE (10 mg/mL)	0.2698±0.0178	0.2173±0.0092***	24.020±2.937***
BLE (15 mg/mL)	0.2835±0.0268	0.1561±0.0059***	41.908±4.488***
BLE (20 mg/mL)	0.2958±0.0103	0.0891±0.0150***	68.701±3.087***

**$p<0.01$ and ***$p<0.001$ indicating the significance of the weight of the clot after lysis compared to the weight of the clot before lysis

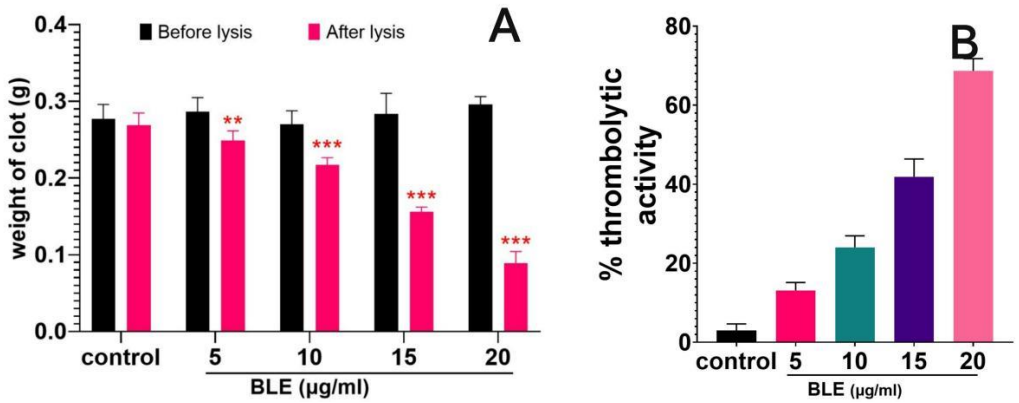

Fig 17: Thrombolytic activity of BLE on chicken blood

A.Effect of BLe on the weight of clot; B. %thrombolytic activity of BLEs

3.17 Molecular Docking for Bambusa Bambos

Molecular docking study results phytocompounds of Bambusa bambos, (24E)-24-N Propylidene cholesterol (-8.9 kcal/mol), 3, 4-Dihydroxybenzoic acid (-6.45 kcal/mol), Chlorogenic acid (-6.4 kcal/mol) showed similar results in comparison to the standard drug, Rivaroxaban which formed 5 hydrogen bonds with the target, Factor X (PDB ID: 1KSN), indicating higher stability than the phytocompounds.

Results of phytocompounds, (24E)-24-N Propylidene cholesterol (-8.27 kcal/mol), Taxiphyllin (-6.24 kcal/mol), Ferulic acid (-6.13 kcal/mol) showed higher interaction with Thrombin (PDB ID: 1KTS) similar to that of the standard drug, Dabigatran. Antithrombin III (PDB ID: 2B4X) had provided targets for (24E)-24-N Propylidene cholesterol (-7.07 kcal/mol), Allantoin (-4.91 kcal/mol), 2, 6-Dimethoxy-1, 4-benzoquinone (-4.89 kcal/mol) with higher affinity similar to clopidogrel. Vitamin-K Epoxide Reductase (PDB ID: 3KP9) also provided targets that showed a higher affinity with (24E)-24-N Propylidene cholesterol (-11.51 kcal/mol), Dibutyl phthalate (-6.53 kcal/mol), 4-Hydroxycinnamic acid (-6.47 kcal/mol). (24E)-24-N Propylidene cholesterol formed 2 hydrogen bonds with the target showing better interaction than the standard, warfarin. Overall, (24E)-24-N Propylidene cholesterol exhibited consistently better binding affinity across all the target receptors showing it as the likely responsible compound in Bambusa bambos for its anticoagulant property.

3.18 MOLECULAR DOCKING FOR DE NOVO DRUG

Based on the docking results 5 models de novo drug had been designed and investigated for the binding affinity for the coagulation receptors as investigated above and compared with the standard drugs. Results showed that the De novo drug model 5 showed the highest binding energy (-7.13 kcal/mol) with Factor X with two hydrogen bonds, comparable to Rivaroxaban. With Thrombin (PDB ID: 1KTS). De novo drug models 4 and 5 showed higher binding energies compared to Dabigatran, but Dabigatran formed more hydrogen bonds, indicating a potentially more stable complex. All de novo drug models exhibited higher binding energies than Clopidogrel with Antithrombin III but lacked in forming the same hydrogen bonds. De novo drug model 5 exhibited the highest binding energy (-8.54 kcal/mol) with Vitamin-K

epoxide reductase forming one hydrogen bond, comparable to Warfarin. Overall, De novo drug model 5 consistently showed promising binding energies and interactions comparable to or better than existing drugs (Rivaroxaban, Dabigatran, Clopidogrel, and Warfarin).

3.19 Drug-Likeness Properties and Toxicity Prediction

Notably, all the designed de novo drug models passed Lipinski's rule of 5, which can be categorized under the predicted toxicity class of 4 and 5. Also, they were inactive for almost all the toxicity endpoints as shown in Fig. 18.

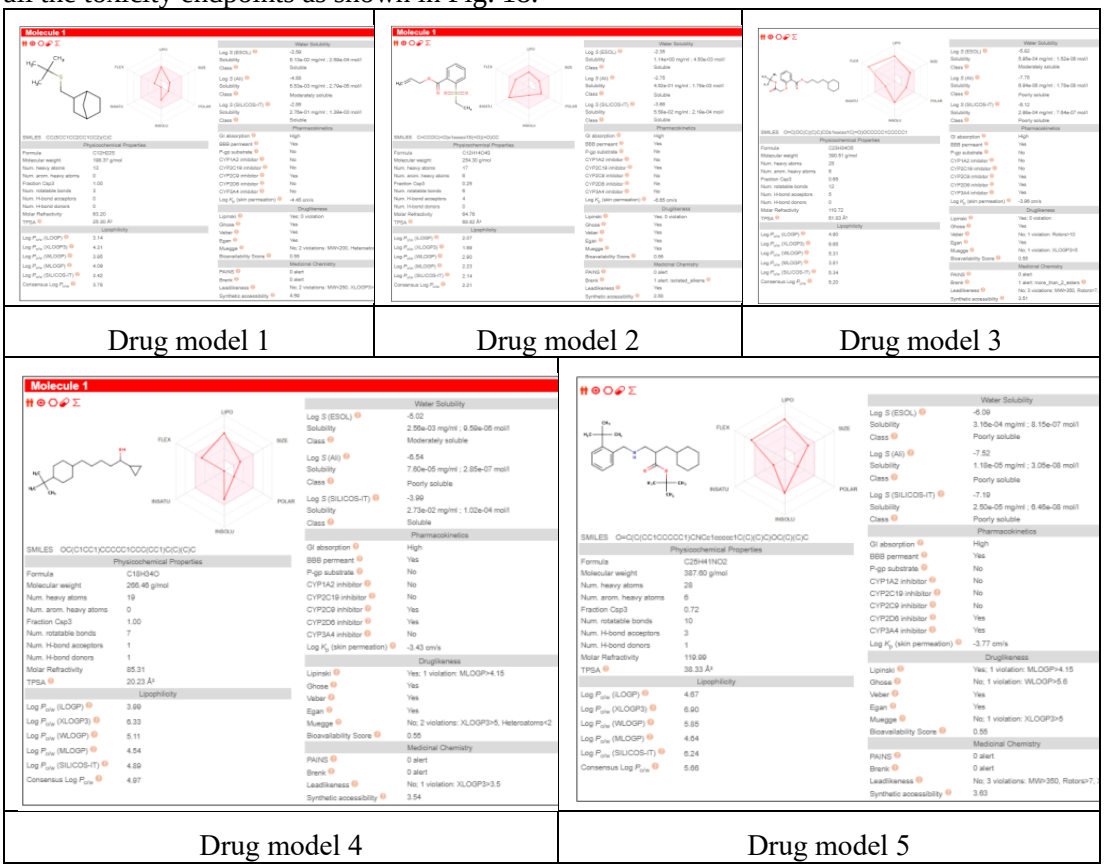

Fig 18: De novo drug model 1, 2, 3, 4 and 5

4. Discussions

Literature highlights the traditional use of Bambusa bambos all over India by tribal people, vaidhiyars, and hakims to treat various physical ailments such as fever, stomach problems, wound healing, kidney diseases, hypertension, stroke, malignant tumours, and gynaecological problems like amenorrhea, oligomenorrhoea, etc.[41] [42] In Siddha literature, it is evident that various Siddha compound medicines like cutakutaippu kutinir curanam and caturmuka kulikai are prepared from Bambusa bambos leaves to cure amenorrhoea, oligomenorrhoea, stroke, and the leaf juice is used as an adjuvant medicine in velvanka centuram to treat malignant tumours.

To provide scientific evidence for the application of Bambusa bambos in the treatment of COVID-19 Vaccination-Associated Coagulopathy, various standardization studies like microscopic examination, histochemical study, DNA barcoding, HPTLC fingerprinting, GC-MS profile, In vitro studies, Molecular Docking studies, and Denova drug models had been carried out for the first time using scientific and standard techniques.

The physicochemical parameters of Bambusa bambos leaf powder were found under Pharmacopeial limits. The microscopic examination showed a very clear strain representing the upper and lower epidermis with covered with numerous cuticular outgrowths. It is supported by a histochemical study showing the presence of cutins in the layers of the epidermis. Alkaloids, plicate cells, and lignin deposition were also observed. The genomic DNA was isolated from the authenticated Bambusa spp. The sample exhibited a concentration of 636.50 ng/µL with an A260/A280 ratio of 2.15, indicating the authenticity and high quality of the plant powder. The therapeutic value of plants is derived from chemical compounds that have a specific physiological function on the human body and most important of them include alkaloids, tannins, flavonoids, and phenolic chemicals [43] that are present in Bambusa.

Free radicals are a major contributing factor to the development of diseases such as hypertension, vascular disorders, and metabolic syndrome. Quercetin, an important bioflavonoid is renowned for its antioxidant, anti-inflammatory, antihypertensive, vasodilator, anti-obesity, anti-hypercholesterolemic, and anti-atherosclerotic properties.[7] [44] The methanol extract of bambusa (BLE) was confirmed to contain quercetin as in Table 3. This supports the assumption that the extract possesses antioxidant activity and can be used to prevent platelet aggregation and lipid peroxidation. The extract also showed potent antioxidant activity in comparison to the standard, ascorbic acid indicating 59.62 µg of BLE was found equivalent to 8.95 µg of standard as shown in figure 11. GC-MS analysis of the extract showed the presence of 33 compounds indicated in Table 4.

There are literature evidence that opportunistic bacterial and fungal infections are widespread in COVID-19 patients admitted to the ICU, with gram-negative bacteria and Candida species being the most prevalent. Invasive mechanical breathing was found to dramatically increase the risk of subsequent infections. Poor clinical results have been reported, including longer hospital and ICU stays and greater mortality. Bacterial resistance to drugs makes treating infectious disorders more challenging. As a result, it is vital to discover alternate treatments for microorganism-caused infections. [45] [46] The treatment of infectious diseases remains a difficult endeavor due to a variety of circumstances, including an alarming increase in the number of multi-drug-resistant microbial infections.[47] The current investigation revealed a potent antibacterial and antifungal activity of BLE on Streptococcus, Bacillus, E.coli, Staph and Pseudomonas bacteria, and Candida and Aspergillus fungi. The activity was potent compared to the standard drugs, Amphotericin and Ciprofloxacin as shown in Table 5.

COVID-19 was proven to cause negative effects on wound healing due to aggravation of inflammation and oxidative stress and deterioration of hematological epidermal stem cell functions thus worsening primary wounds and delaying healing.[48] MTT assay conducted on HaCaT cell lines showed the IC_{50} value of the extract as 64.35 µg/mL and induced toxicity at 250 µg/mL in the cell line. Wound healing activity on the HaCaT cell lines indicated that the treatment with BLE showed better wound healing in the scratch assay compared to the control

cells with 33% better healing as in Table 6. The in vitro HaCaT cell lines in Fig. 14 indicated a positive effect of the treatment on cell healing, with the treated cells showing greater gap closure compared to the control.

Studies concluded that there is a direct relation of thrombosis with COVID-19 leading to mortality of the patients.[2] Thrombosis in COVID-19 is a result of inflammation in the endothelium of the vascular tissue due to infection.[8] Thus in the current investigation, chicken blood was treated with Bambusa leaf extract at different concentrations like 5, 10, 15, and 20 mg/mL showed a significant increase in anticoagulant activity, antithrombolytic activity, and prothrombin inhibition activity.

Molecular mechanisms indicate that thrombosis is caused due to the dissemination of intravascular coagulation and platelet fibrin thrombus deposition.[9] Activation of macrophages and cytokines remain as inflammatory causes of thrombus formation.[10] Also, Studies showed that COVID-19 causes variations of prothrombin and partial thromboplastin time resulting in thrombus formation.[11] Thus molecular docking was conducted to evaluate various phytocompounds from Bambusa bambos against different target proteins like Factor X (PDB ID: 1KSN), Thrombin (PDB ID: 1KTS), Antithrombin III (PDB ID: 2B4X) and Vitamin-K epoxide reductase (PDB ID: 3KP9), comparing their efficacy to standard drugs like Rivaroxaban, Dabigatran, Clopidogrel, and Warfarin. As a result, (24E)-24-N Propylidene cholesterol could be a promising lead compound for further investigation due to its strong interactions with target proteins, potentially acting as an efficient anticoagulant compared to standard drugs. The De novo drugs were designed using the WADDAICA web server and subsequently docked with target proteins as above. De novo drug model 5 ((24E)-24-N-Propylidenecholesterol.) consistently showed promising binding energies and interactions comparable to or better than existing drugs (Rivaroxaban, Dabigatran, Clopidogrel, and Warfarin).

Hence the mechanisms of the drugs can be explained in terms of their activity in interacting with Factor X, which is important in the clotting of blood. An increase in clotting factor X results in a hypercoagulable state leading to thrombosis and thromboembolism.[49] By inhibiting the receptor, it is clear that the chemical compounds in Bambusa bambos prevent clot formation as evident in the molecular docking results in Table 9. Thrombin plays an important role in clotting of blood by enhancing platelet aggregation and adhesion. The activation of the thrombin enzyme results in the cleavage of fibrinogen into fibrin that is converted into a clot resulting in a hemostatic plug.[50] Thus inhibition of thrombin is also one of the major mechanisms that is responsible for the high potency of the extract of Bambusa bambos in exhibiting the anticoagulant activity. The results of anticoagulant activity and thrombolytic activity in Tables 7 and 8 and molecular docking results in Table 10 indicate that the thrombolytic activity of the extract and inhibiting the thrombin receptor might be the mechanisms for the activity of the extract.

Antithrombin-III is a plasma glycoprotein that consists of 432 amino acids that inhibit the coagulation process by inhibiting the activity of factors IX and X.[51] The mechanism of clotting by thrombin and factor X was as discussed above. The deficiency or under function of the antithrombin receptor is directly linked to thrombosis and thromboembolism.[52] Thus the mechanism of the anticoagulant activity of the Bambusa bambos extract can be elucidated

and asserted by inhibiting the antithrombin receptor as discussed in Table 11. Previous investigations showed that Vitamin K epoxide reductase (VKOR) is an important enzyme for Vit-K-based carboxylation which is necessary for the coagulation of blood. On the other hand, VKOR is the primary target for warfarin, in the presence of warfarin, the increase in the reduced Vit-K is hindered thus preventing clot formation.[53] In our study, the chemical compounds in the extract of Bambusa bambos significantly inhibited the VKOR receptor similar to the warfarin. Thus, it can be inferred that the anticoagulant activity of Bambusa bambos is due to the inhibition of factor X, thrombin, and VKOR receptors and also by interaction with antithrombin III. De novo drug models also showed significant activity in interacting with all the receptors. Among them, model 3 showed better interaction and affinity to the receptors. Thus, our study supports the traditional medical claims of the Bambusa bambos plant as an anticoagulant to prevent thrombosis and thromboembolism and claims of antibacterial and antiviral properties that improve the health of normal patients and lower the mortality of COVID-19 patients.

5. Conclusion

The current study proved the anticoagulant, thrombolytic, antibacterial, antifungal, and antioxidant activities of methanol extract of leaves of Bambusa bambos. The study provides scientific evidence for the activities. On the other hand, this study also focuses on the standardization of the plant material for macroscopical and microscopical characters, and phytochemical analysis using advanced techniques like HPTLC, GC-MS, and also DNA barcoding. This work is an attempt to support traditional drugs for their therapeutic effect, to elucidate the exact mechanism of action, and to establish the interactions of the drug to the receptors responsible for the activity. Further research is needed to isolate the herbal lead molecule that shows potent anticoagulant activity and to establish the plant as a drug of choice for thromboprophylaxis in COVID-19 patients. To confirm these findings and to investigate the potential uses of these phytocompounds in medical therapies, additional research in clinical trials on Siddha compounds is essential.

Declaration of Generative AI and AI-assisted technologies in the writing process

During the preparation of this work, the authors used an artificial intelligence-assisted WADDAICA tool. After using this tool/service, the author (s) reviewed and edited the content as needed and took full responsibility for the content of the publication.

Acknowledgements

The authors are thankful to the Honourable Vice Chancellor, SASTRA Deemed University, Thanjavur, and the Department of Pharmacognosy and Chemistry, Siddha Central Research Institute, Chennai for providing the infrastructure to carry out the research work.

References

1. Worldometers COVID Live—Coronavirus Statistics—Worldometer. [Accessed on 16 December 2022]. Available online: https://www.worldometers.info/coronavirus/
2. Elezkurtaj S., Greuel S., Ihlow J., Michaelis E.G., Bischoff P., Kunze C.A., Sinn B.V., Gerhold

M., Hauptmann K., Ingold-Heppner B., et al. Causes of Death and Comorbidities in Hospitalized Patients with COVID-19. Sci. Rep. 2021;11:4263. doi: 10.1038/s41598-021-82862-5.
3. Iba T, Levy JH, Connors JM, Warkentin TE, Thachil J, Levi M. The unique characteristics of COVID-19 coagulopathy. Crit Care. 2020;24(1):360.
4. Helms J, Tacquard C, Severac F, et al; CRICS TRIGGERSEP Group (Clinical Research in Intensive Care and Sepsis Trial Group for Global Evaluation and Research in Sepsis). High risk of thrombosis in patients with severe SARS-CoV-2 infection: a multicenter prospective cohort study. Intensive Care Med. 2020;46(6):1089-1098.
5. Suh, Y.J.; Hong, H.; Ohana, M.; Bompard, F.; Revel, M.-P.; Valle, C.; Gervaise, A.; Poissy, J.; Susen, S.; Hékimian, G.; et al. Pulmonary Embolism and Deep Vein Thrombosis in COVID-19: A Systematic Review and Meta-Analysis. Radiology 2021, 298, E70–E80.
6. Wichmann D., Sperhake J.-P., Lütgehetmann M., Steurer S., Edler C., Heinemann A., Heinrich F., Mushumba H., Kniep I., Schröder A.S., et al. Autopsy Findings and Venous Thromboembolism in Patients with COVID-19. Ann. Intern. Med. 2020;173:268–277. doi: 10.7326/M20-2003.
7. Mani A, Ojha V. Thromboembolism after COVID-19 Vaccination: A Systematic Review of Such Events in 286 Patients. Ann Vasc Surg. 2022 Aug;84:12-20.e1. doi: 10.1016/j.avsg.2022.05.001.
8. Peerschke E.I., Yin W., Ghebrehiwet B. Complement activation on platelets: implications for vascular inflammation and thrombosis. Mol Immunol. 2010;47(13):2170–2175.
9. Tang N., Li D., Wang X., Sun Z. Abnormal coagulation parameters are associated with poor prognosis in patients with novel coronavirus pneumonia. J Thromb Haemostasis. 2020;18(4):844–847.
10. Hanff T.C., Mohareb A.M., Giri J., Cohen J.B., Chirinos J.A. Thrombosis in COVID-19. Am J Hematol. 2020;95(12):1578–1589.
11. Cipolloni L., Sessa F., Bertozzi G., Baldari B., Cantatore S., Testi R., et al. Preliminary post-mortem COVID-19 evidence of endothelial injury and factor VIII hyperexpression. Diagnostics. 2020;10(8):575.
12. Malas, M.B., Naazie, I.N., Elsayed, N., Mathlouthi, A., Marmor, R. and Clary, B., 2020. Thromboembolism risk of COVID-19 is high and associated with a higher risk of mortality: a systematic review and meta-analysis. EClinicalMedicine, 29.100639.
13. Fuzimoto A.D., Isidoro C. The antiviral and coronavirus-host protein pathways inhibiting properties of herbs and natural compounds-Additional weapons in the fight against the COVID-19 pandemic? J Tradit Complement Med. 2020;10(4):405–419.
14. Singh N.A., Kumar P., Kumar N. Spices and herbs: potential antiviral preventives and immunity boosters during COVID-19. Phytother Res. 2021;35:2745–2757.
15. Panyod S., Ho C.-T., Sheen L.-Y. Dietary therapy and herbal medicine for COVID-19 prevention: a review and perspective. J Tradit Complement Med. 2020;10(4):420–427.
16. Ang L., Lee H.W., Kim A., Lee M.S. Herbal medicine for the management of COVID-19 during the medical observation period: a review of guidelines. Integr Med Res. 2020;9(3):100465.
17. Shahzad F., Anderson D., Najafzadeh M. The antiviral, anti-inflammatory effects of natural medicinal herbs and mushrooms and SARS-CoV-2 infection. Nutrients. 2020;12(9):2573.
18. Gautam S., Gautam A., Chhetri S., Bhattarai U. Immunity against COVID-19: potential role of Ayush Kwath. J Ayurveda Integr Med. 2022;13(1):100350.
19. Johansen D.A. 1940 Plant Microtechnique. McGraw Hill Book Co; New York Pp.523.
20. O'Brien, P.Feder N. and Mc Cull M.E. 1964. Polychromatic staining of plant cell walls by toulidine blue-O protoplasma; 59:364-373
21. Shabouri EI MI. Positively charged nanoaprticles for the oral bioavailability of cyclosporine-

A. Int J Pharm 2003;249:101-08.
22. Kaneria, M., Kanani, B., & Chanda, S. (2012). Assessment of effect of hydroalcoholic and decoction methods on extraction of antioxidants from selected Indian medicinal plants. Asian Pacific journal of tropical biomedicine, 2(3), 195–202.
23. Harborne, Methods of Extraction and Isolation, in: Phytochemical methods, third ed., Chapman and Hall, London, 1998, pp. 60-66.
24. Lee Y.H., Choo C., Watawana M.I., Jayawardena N., Waisundara V.Y. An appraisal of eighteen commonly consumed edible plants as functional food based on their antioxidant and starch hydrolase inhibitory activities. J. Sci. Food Agric. 2015;95:2956–2964. doi: 10.1002/jsfa.7039.
25. Aryal S, Baniya MK, Danekhu K, Kunwar P, Gurung R, Koirala N. Total Phenolic Content, Flavonoid Content and Antioxidant Potential of Wild Vegetables from Western Nepal. Plants (Basel). 2019 Apr 11;8(4):96. doi: 10.3390/plants8040096. PMID: 30978964; PMCID: PMC6524357.
26. Medini F, Fellah H, Ksouri R, Abdelly C. Total phenolic, flavonoid and tannin contents and antioxidant and antimicrobial activities of organic extracts of shoots of the plant Limonium delicatulum. Journal of Taibah University for science. 2014 Jul 1;8(3):216-24.
27. Raman V, Budel JM, Zhao J, Bae JY, Avula B, Osman AG, Ali Z, Khan IA. Microscopic characterization and HPTLC of the leaves, stems and roots of Fadogia agrestis-an African folk medicinal plant. Revista Brasileira de Farmacognosia. 2018 Dec;28:631-9.
28. Gomathi D, Kalaiselvi M, Ravikumar G, Devaki K, Uma C. GC-MS analysis of bioactive compounds from the whole plant ethanolic extract of Evolvulus alsinoides (L.) L. J Food Sci Technol. 2015 Feb;52(2):1212-7. doi: 10.1007/s13197-013-1105-9.
29. Konappa, N., Udayashankar, A.C., Krishnamurthy, S. et al. GC–MS analysis of phytoconstituents from Amomum nilgiricum and molecular docking interactions of bioactive serverogenin acetate with target proteins. Sci Rep 10, 16438 (2020). https://doi.org/10.1038/s41598-020-73442-0
30. Christenson, J. C., Korgenski, E. K., & Relich, R. F. (2018). Laboratory Diagnosis of Infection Due to Bacteria, Fungi, Parasites, and Rickettsiae. In S. S. Long, C. G. Prober, & M. Fischer (Eds.), Principles and Practice of Pediatric Infectious Diseases (5th ed., pp. 1422-1434.e3). Elsevier. ISBN: 9780323401814.
31. Abdulrasheed-Adeleke, T. & Bola, B. (2020). Comparative in vitro antioxidant activities of aqueous extracts of Garcinia kola and Buchholzia coriacea seeds. Tanzania Journal of Science, 46, 498-507.
32. Imam, M.Z., et al. (2011). Antioxidant activities of different parts of Musa sapientum L. ssp. sylvestris fruit. Journal of Applied Pharmaceutical Science, 1, 68-72.
33. Kaneria, M., et al. (2012). Assessment of effect of hydroalcoholic and decoction methods on extraction of antioxidants from selected Indian medicinal plants. Asian Pacific Journal of Tropical Biomedicine, 2(3), 195–202.
34. Morgan DML. Tetrazolium (MTT) assay for cellular viability and activity. Methods Mol Biol. 1998; 79:179-84.
35. Van Meerloo J, Kaspers GJL, Cloos J. Cell sensitivity assays: The MTT assay. Methods Mol Biol. 2011; 731: 237-45.
36. Prabhath, Sushma & Bhat, Kumar & Padma, Divya & Pai K, Sreedhara. (2019). Influence of traditional medicines on the activity of keratinocytes in wound healing: an in-vitro study. Anatomy & Cell Biology. 52. 10.5115/acb.19.009.
37. Borela, V.T., Balunsat, K.A.L., Briones, A.J.L. and Briones, P.N.P., 2020. In-Vitro study of the Anticoagulant Property of Terminalia Catappa (Talisay) Leaf Extract Using Gallus Gallus (Chicken) Blood. Journal La Lifesci, 1(3), pp.25-29.
38. Ayodele, O.O., Onajobi, F.D. and Osoniyi, O., 2019. In vitro anticoagulant effect of

Crassocephalum crepidioides leaf methanol extract and fractions on human blood. Journal of experimental pharmacology, pp.99-107.

39. Chaudhary, S., Godatwar, P.K. and Sharma, R., 2015. In vitro thrombolytic activity of Dhamasa (Fagonia arabica Linn.), Kushta (Saussurea lappa Decne.), and Guduchi (Tinospora cordifolia Thunb.). AYU (An international quarterly journal of research in Ayurveda), 36(4), pp.421-424. DO: 10.4103/0974- 8520.190697
40. Hussain, F., Islam, A., Bulbul, L., Moghal, M.R. and Hossain, M.S., 2014. In vitro thrombolytic potential of root extracts of four medicinal plants available in Bangladesh. Ancient science of life, 33(3), pp.162-16
41. Lodhi S, Jain AP, Rai G, Yadav AK. Preliminary investigation for wound healing and anti-inflammatory effects of Bambusa vulgaris leaves in rats. J Ayurveda Integr Med. 2016 Mar;7(1):14-22. doi: 10.1016/j.jaim.2015.07.001. Epub 2016 Apr 11. PMID: 27297505; PMCID: PMC4910292.
42. Tomar, B.; Anders, H.-J.; Desai, J.; Mulay, S.R. Neutrophils and Neutrophil Extracellular Traps Drive Necroinflammation in COVID-19. Cells 2020, 9, 1383. https://doi.org/10.3390/cells9061383
43. Okwu D.E. (2001), "Evaluation of The Chemical Composition of Indigenous Spices and Flavouring Agents", Global J. Pure Appl. Sci. 7(3), 455-459.
44. Lekakis J, Rallidis LS, Andreadou I, Vamvakou G, Kazantzoglou G, Magiatis P, et al. Polyphenolic compounds from red grapes acutely improve endothelial function in patients with coronary heart disease. Eur J Cardiovasc Prev Rehabil. 2005;12:596–600.
45. Rajeev Kurele. Drug standardization of ayurvedha, unani and siddha drugs. Int. J. Res. Ayurveda Pharm, 2015; 6(2): 192-194.
46. Batiha G.E., Beshbishy A.M., Ikram M., Mulla Z.S., El-Hack M.E.A., Taha A.E., Algammal A.M., Elewa Y.H.A. The Pharmacological Activity, Biochemical Properties, and Pharmacokinetics of the Major Natural Polyphenolic Flavonoid: Quercetin. Foods. 2020;9:374. doi: 10.3390/foods9030374.
47. Alshrefy AJ, Alwohaibi RN, Alhazzaa SA, Almaimoni RA, AlMusailet LI, AlQahtani SY, Alshahrani MS. Incidence of Bacterial and Fungal Secondary Infections in COVID-19 Patients Admitted to the ICU. Int J Gen Med. 2022 Sep 24; 15:7475-7485. doi: 10.2147/IJGM.S382687.
48. Li, D., Cao, W., Zhou, Q., Wu, X., Song, X. and Qin, H., 2023. COVID-19 and primary wound healing: A new insights and advance. International Wound Journal, 20(10), pp.4422-4428.
49. Brown D.L., Koides P.A. Diagnosis and treatment of inherited factor X deficiency. Haemophilia. 2008;14:1176–1182.
50. Al-Amer OM. The role of thrombin in haemostasis. Blood Coagul Fibrinolysis. 2022 Apr 1;33(3):145-148. doi: 10.1097/MBC.0000000000001130.
51. Hsu E, Moosavi L. Biochemistry, Antithrombin III. [Updated 2023 Sep 4]. In: StatPearls [Internet]. Treasure Island (FL): StatPearls Publishing; 2024 Jan-. Available from: https://www.ncbi.nlm.nih.gov/books/NBK545295/#
52. Bravo-Pérez C, Vicente V, Corral J. Management of antithrombin deficiency: an update for clinicians. Expert Rev Hematol. 2019 Jun;12(6):397-405.
53. Wu, S., Chen, X., Jin, D.Y., Stafford, D.W., Pedersen, L.G. and Tie, J.K., 2018. Warfarin and vitamin K epoxide reductase: a molecular accounting for observed inhibition. Blood, The Journal of the American Society of Hematology, 132(6), pp.647-657.